buildings

MDPI

Article

The Effect of the Isolation Hotel Facade Attachment on the Inter-Flat Transmission of Aerosols

Nan Zhang [1], Yuze Li [1], Ying Ji [1] and Xiangyu Li [2,*]

[1] Beijing Key Laboratory of Green Built Environment and Energy Efficient Technology, Beijing University of Technology, Beijing 100124, China; zhangn@bjut.edu.cn (N.Z.); liyuze@emails.bjut.edu.cn (Y.L.); jiying@bjut.edu.cn (Y.J.)
[2] School of Architecture & Design, China University of Mining and Technology, Xuzhou 221116, China
* Correspondence: 6788@cumt.edu.cn; Tel.: +86-13671006582

Abstract: Although natural ventilation can effectively control the indoor air quality and thermal comfort, the single-sided natural ventilation in isolation hotels may lead to the transmission of virus-laden aerosols between windows on the same façade but on different floors near the pollution source. Hereinafter, this kind of transmission is referred to as inter-flat transmission. The configuration of the building façade is a key factor influencing this risk. This study took into account various façade attachment scenarios including flat façades (with no attachments), outdoor units only, awnings only, and a combination of outdoor units and awnings. A model based on a real isolation hotel was developed, and computational fluid dynamics (CFD) simulations were carried out to investigate the inter-flat transmission of aerosols under these façade conditions. The study analyzed the risk of gaseous pollutant transmission caused by single-sided natural ventilation and quantified the effects of different outdoor wind speeds and indoor–outdoor temperature differences on this transmission route. When the indoor–outdoor temperature difference was 5 °C, the mass fraction of gaseous pollutants in the receptor rooms above the source first increased and then decreased as the outdoor wind speed increased, reaching a peak at 1 m/s. When the outdoor wind speed was 2 m/s, the mass fraction of pollutants in the receptor rooms increased with the increase in the indoor–outdoor temperature difference. Compared with the flat façade, the presence of outdoor units reduced the air exchange rate of natural ventilation, resulting in a slight increase in the infection risk. A 1 m-long awning reduced the infection risk associated with inter-flat transmission by 46%. Buildings equipped with both a 1 m-long awning and outdoor units achieved a 68% reduction in infection risk. These findings provide valuable insights for mitigating inter-flat transmission and inform the development of relevant policies.

Keywords: isolation hotel; inter-flat transmission; airborne transmission; façade attachment; ventilation

check for updates

Received: 14 January 2025
Revised: 22 February 2025
Accepted: 24 February 2025
Published: 25 February 2025

Citation: Zhang, N.; Li, Y.; Ji, Y.; Li, X. The Effect of the Isolation Hotel Facade Attachment on the Inter-Flat Transmission of Aerosols. *Buildings* **2025**, *15*, 755. https://doi.org/10.3390/buildings15050755

Copyright: © 2025 by the authors. Licensee MDPI, Basel, Switzerland. This article is an open access article distributed under the terms and conditions of the Creative Commons Attribution (CC BY) license (https://creativecommons.org/licenses/by/4.0/).

1. Introduction

Isolation hotels, which were specifically designated for quarantining incoming travelers during the COVID-19 pandemic, have been widely established in various regions around the world. Quarantined individuals were required to stay in their assigned rooms within the isolation hotel for 2–3 weeks without any contact with others [1]. However, due to the lack of understanding of the transmission pathways of COVID-19 within isolation hotels, outbreaks were reported in such facilities during the pandemic in several countries including Canada [2], New Zealand [3], China [4,5], and Australia [6].

By 15 June 2021, 22 outbreaks had occurred in isolation hotels in Australia. Outbreaks in two Melbourne isolation hotels triggered Victoria's second wave of infections, resulting in nine lockdowns across the state and approximately 800 deaths [6]. On 1 November 2021, an isolation hotel in Changping District, Beijing, China experienced a family cluster outbreak caused by virus transmission through ventilation ducts, which belong to long-range transmission, during the quarantine period [7]. The high density of potentially infected individuals in isolation hotels, combined with the fact that most of these facilities were not originally designed for epidemic prevention and lacked adequate measures to control aerosol transmission within buildings, poses a significant risk of respiratory infectious diseases.

In isolation hotels, natural ventilation not only helps improve indoor air quality, but also assists in controlling thermal comfort, creating a favorable indoor environment for residents. The airflow in natural ventilation is generated by the pressure difference between the indoors and outdoors. In single-sided natural ventilation, the temperature difference and wind pressure difference between the interior and exterior drive air exchange, which is crucial for the spread of pollutants. This air transmission is related to buoyancy, wind force, and their combined effects [8]. In the absence of wind, the warm air at the lower level will flow or mix with the external gas and then rise to the upper level. When buoyancy dominates in multi-story buildings, a "cascade" effect occurs, leading to the transmission of pollutant gases from the lower floors to the upper rooms.

Single-sided natural ventilation may lead to the inter-flat transmission of pollutants across floors. Under the combined effects of wind pressure and thermal pressure [9], pollutants can spread from lower-floor rooms to upper-floor rooms through open windows, resulting in cross-contamination. During the SARS outbreak in Hong Kong, a special air transmission route was identified, known as inter-flat transmission or "vertical transmission". This refers to cross-infection between different floors of the same building, a phenomenon that occurs under single-sided natural ventilation. Through epidemiological analysis, experiments, and airflow simulations, Li et al. [3] conducted further research on the largest-scale outbreak in a luxury residential building and a hospital, analyzing the leakage of viruses through external windows.

Liu et al. [10] investigated the mechanisms and effects of outdoor vertical transmission under single-sided natural ventilation in high-rise buildings using numerical simulations. Field measurements revealed that under single-sided natural ventilation, up to 7% of the indoor air in the upper-floor rooms originated directly from the lower-floor rooms, indicating a risk of cross-infection [11]. Wang et al. [12] examined the transmission of gaseous pollutants through windows during single-sided natural ventilation in multi-story buildings. They used CFD to simulate the pollutant dispersion for six different window configurations, uncovering the effects of ventilation rates and temperature fields on pollutant transmission.

All in all, although single-sided natural ventilation has advantages in terms of energy efficiency and thermal comfort, its application in isolation hotels brings a significant risk of cross-infection.

Currently, studies on single-sided ventilation mainly rely on experimental measurements and numerical simulations to calculate the amount of pollutants discharged from the source rooms that re-enter other indoor environments, thereby quantifying the possibility of cross-transmission. Since the wind pressure difference along the flat façade affects inter-flat transmission, the attachments on the building façade may change the airflow patterns, thus affecting the transmission paths and concentration distribution of pollutants. However, research on the impact of façade attachments on the vertical transmission of gaseous pollutants outside buildings is still limited.

This study analyzed the impact of the façade attachments of isolation hotels on the virus aerosol transmission caused by single-sided natural ventilation. Taking a real isolation hotel in China as a model, four scenarios were studied: a flat façade with no attachments, a façade with only outdoor units, only awnings, and a combination of outdoor units and awnings. Through CFD simulations, the pollutant transmission inside and outside the multi-story building was studied, the transmission characteristics under single-sided natural ventilation were analyzed, and the effects of outdoor wind speed and indoor–outdoor temperature differences on the transmission path were quantified. The results of this study contribute to the prevention and control of outdoor vertical transmission in buildings and provide a reference for the development of relevant policies.

2. Method

2.1. Geometrical Model

This study established a multi-story building model based on a real isolation hotel in northern China to simulate the single-sided natural ventilation of gaseous pollutants using CFD. The building has a height H = 15 m, width W = 3 m, and length L = 14 m. The computational domain extends 5 H upstream, 10 H downstream, and has a width of W. The velocity distribution at the domain's inlet in the x-direction follows a logarithmic profile $\left(U(y) = U_0\left(\frac{y}{10}\right)^{0.2}\right)$, with velocity components in the y and z directions set to zero. The boundary conditions for the external flow field are shown in Figure 1a. The building comprises five floors, with a single vertical column of units, and only single-sided rooms were considered. Carbon dioxide was used as the pollutant [12],released at a rate of 3 mL/s, from a point at a height of 1.7 m in the center of the third-floor room, The pollutant was monitored in rooms on the fourth and fifth floors. Façade attachments included awnings and an outdoor unit (Figure 1b).

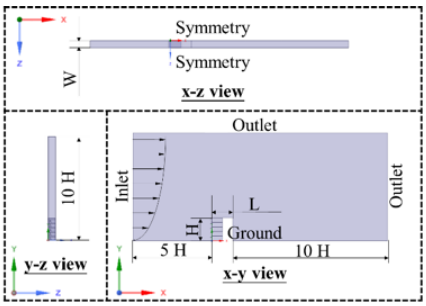

(**a**)

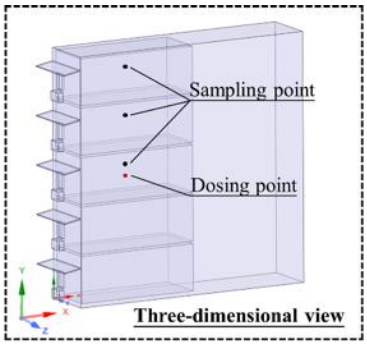

(**b**)

Figure 1. The building geometry model setup for the CFD simulation: (**a**) Computational domain; (**b**) building model.

This study took into account four different façade configurations: flat façade (FF), façade with only outdoor units (OU), façade with only 1 m-long awnings (AN), and

façade with both outdoor units and 1 m-long awnings (AN + OU) (Figure 2). Each room had a window measuring 0.5 m × 0.9 m, and this window remained fully open during the simulation. The outdoor unit was installed directly beneath the window, with its dimensions being 0.8 m × 0.3 m × 0.5 m. The width of the awning was equal to that of a single room (3 m), and it had a certain overhang length L_A. In the simulation, L_A varied between 0.5 m and 1.5 m, and the awning formed an angle of 10° with the horizontal plane.

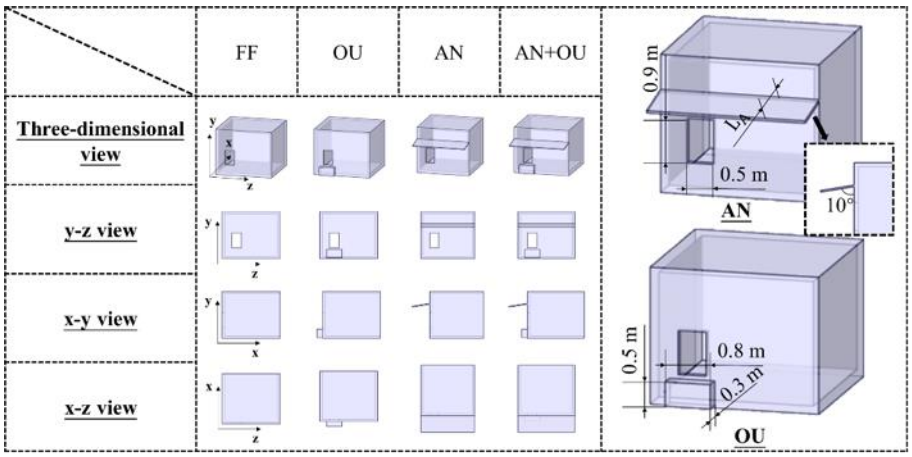

Figure 2. Façade configurations and dimensions of the building attachments.

2.2. Governing Equations

The airflow and pollutant transport inside and outside the multi-story building were characterized by solving the governing equations of fluid flow, heat transfer, and scalar transport. Since these equations are widely available in the Fluent User's Guide (ANSYS Inc., USA, Fluent 16.0 User's Guide, Canonsburg, 2015), a brief summary of the governing equations used in this study is provided below. The continuity, momentum, and energy equations for incompressible fluids are as follows:

$$\vec{\nabla} \cdot \vec{u} = 0 \tag{1}$$

$$\rho\left(\frac{\partial \vec{u}}{\partial t} + \vec{u} \cdot \vec{\nabla}\vec{u}\right) = -\vec{\nabla}p + \mu\vec{\nabla}^2\vec{u} + \rho\vec{g} \tag{2}$$

$$\frac{\partial T}{\partial t} + \vec{u} \cdot \vec{\nabla}T = \frac{K}{\rho c_p}\vec{\nabla}^2 T \tag{3}$$

where $\vec{u}$ is the velocity vector, p is the pressure (N), T is the temperature (°C), K is the thermal conductivity (W/(m·K)), $\vec{g}$ is the gravitational acceleration (m/s^2), ρ is the density (kg/m^3), and μ is the dynamic viscosity (Pa·s). The Boussinesq model was used to account for buoyancy effects caused by variations in air density, approximating the buoyancy term in Equation (2) as the following expression:

$$\rho\vec{g} = \rho_{\text{ref}}\left[1 - \beta(T - T_{\text{ref}})\right]\vec{g} \tag{4}$$

where ρ_{ref} is the reference density, T_{ref} is the reference temperature, and β is the thermal expansion coefficient.

Considering the uncertainties and instabilities during the formulation of the turbulence model, the low Reynolds number RNG k-ε model was adopted. The convection terms were discretized using the second-order upwind scheme, while the diffusion terms were discretized by means of the second-order central difference scheme. The pressure–velocity coupling method employed was the SIMPLE algorithm [13]. The flow characteristics in-

volved in this study included natural convection flow inside cavities and forced convection flow around blunt bodies.

Based on the airflow predicted by the above mathematical model, the equations were further solved to obtain the transmission characteristics of pollutants in both indoor and outdoor environments. For gaseous pollutants like carbon dioxide, which have a similar density to air and are assumed to move with the airflow, the Eulerian method can be used to describe the diffusion and mixing of pollutants in the fluid more effectively. The following scalar transport equation was used to model the transmission of pollutants:

$$\vec{\nabla} \cdot \left(\rho \vec{u} C\right) = \vec{\nabla} \cdot \left(\Gamma_C \vec{\nabla} C\right) + S_C \quad (5)$$

where C is the carbon dioxide concentration, S_C is the source term, and Γ_C is the scalar diffusion rate proposed by Zhang et al. [14] where when the Schmidt number S_t = 10, $\Gamma_C = (\mu + \mu_t)/S_t$. More equations related to scalar transport can be found in the User Manual (ANSYS Inc., Fluent 16.0 User's Guide, Canonsburg, 2015).

2.3. Numerical Solution and Model Validation

To verify the accuracy of the above model, the simulation results of natural ventilation and forced convection were compared with two experimental datasets from the literature. One dataset [15] (hereinafter referred to as Experiment 1) provided the velocity and temperature distribution maps, which were applied to validate the accuracy of the computational fluid dynamics (CFD) model in predicting natural ventilation. The other field-measured experiment (hereinafter referred to as Experiment 2) provided tracer gas profile maps inside a building with buoyancy-driven natural ventilation, which were applied to validate the pollutant transmission model in this study.

2.3.1. Natural Ventilation Within the Cavity

In Experiment 1, the two chambers represent the indoor and outdoor environments, respectively (Figure 3a). The buoyancy-driven natural ventilation was generated by a heater inside the laboratory, with a rectangular opening opposite the heater. There were five measurement points (P1–P5) inside and outside the laboratory to measure the wind speed and temperature. The experimental data from two points (P2 and P5) were used for the validation of the computational fluid dynamics (CFD) model. Figure 3b,c compares the predicted velocity and temperature curves with the experimental data from P2 and P5. As shown in the figures, the velocity and temperature curves matched the experimental data well. Therefore, this provided an acceptable reference for the airflow and temperature distribution of the computational fluid dynamics (CFD) model of the buoyancy-driven natural ventilation.

2.3.2. Pollutant Transmission Resulting from Single-Sided Natural Ventilation

Field measurements regarding the tracer gas simulations were carried out in a COVID-19 isolation hotel located in North China from 8 to 22 April 2024. SF6 was adopted as the tracer gas to mimic the transmission of viral aerosols among the rooms in the hotel. During the measurement period, the outdoor temperature fluctuated between 11.4 °C and 22.7 °C, while the indoor temperature ranged from 13.6 °C to 21.5 °C. All the east-facing rooms (50 rooms in total) of the building were rented for this study. SF6, serving as the tracer gas to simulate gaseous pollutants, was released at a rate of 3 mL/s in Room 303 on the third floor, and its presence was detected in the rooms directly above, namely Room 403 on the fourth floor and Room 503 on the fifth floor (Figure 4a). An experiment was conducted using a six-channel gas collection instrument (model INNOVA 1409, LumaSence, USA; gas

concentration range: 5×10^{-8}), which enabled the simultaneous measurement of tracer gas concentrations at up to six locations. The concentrations of SF6 were extracted from the geometric centers of Rooms 303, 403, and 503.

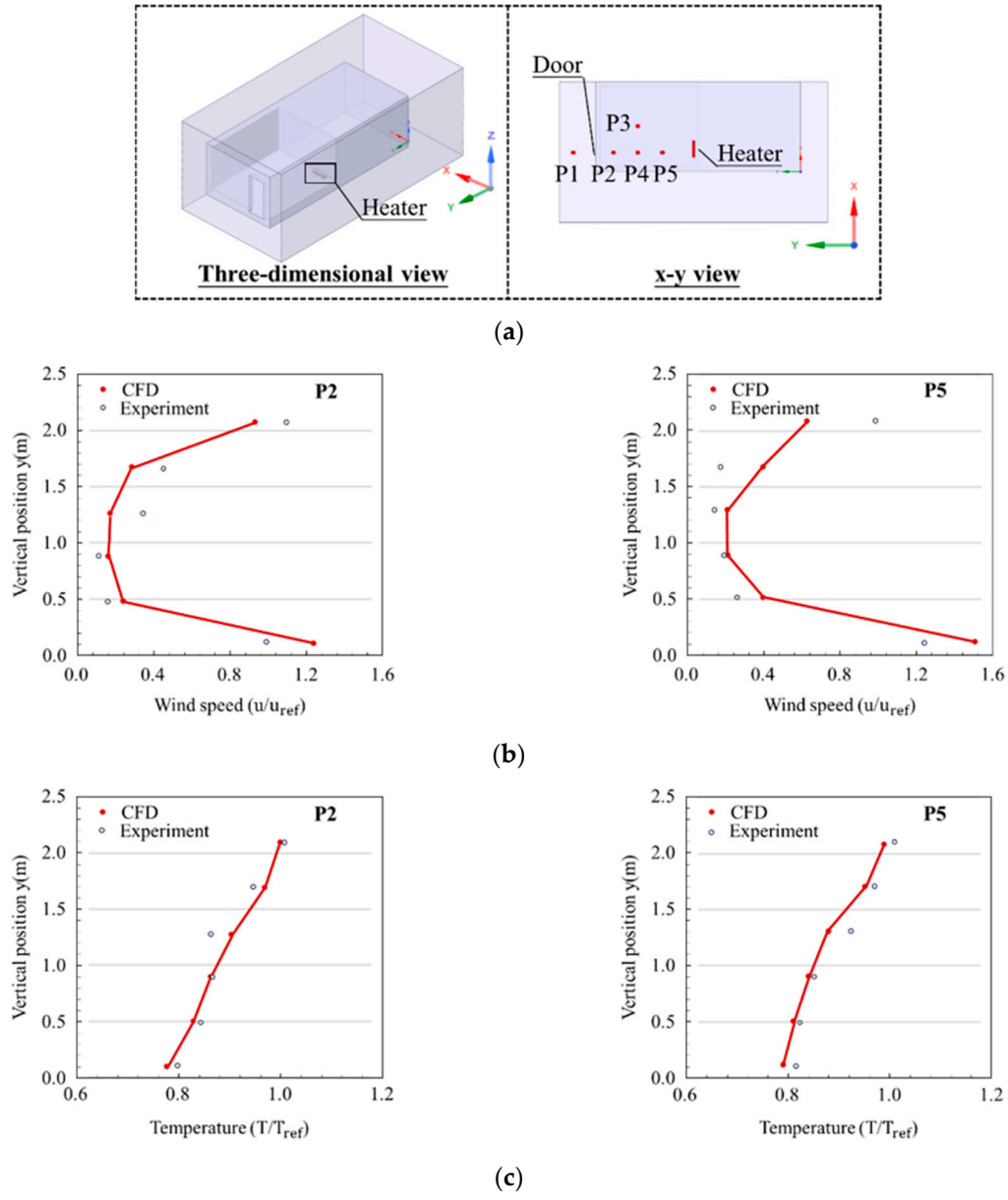

Figure 3. Model setup and validation. (**a**) Model cavity setup; (**b**) comparison of the velocity simulation results of P2 and P5 with the experimental results; (**c**) comparison of the temperature simulation results of P2 and P5 with the experimental results.

CO_2 was utilized as a tracer gas to measure the ventilation rate in each room when the windows were fully open. A carbon dioxide concentration recorder (model TJHY-WEZY-1, TianJian HuaYi, China; gas concentration range: 1 ppm–10,000 ppm) was employed to measure the CO_2 concentration in the rooms. The releases were carried out in the morning, afternoon, and evening, respectively.

A high-precision three-dimensional ultrasonic anemometer (model Wind Master with a 20 Hz output, made by GILL, UK; having a wind speed range of 0–65 m/s) was used to detect the airflow in the localized areas of the external walls.

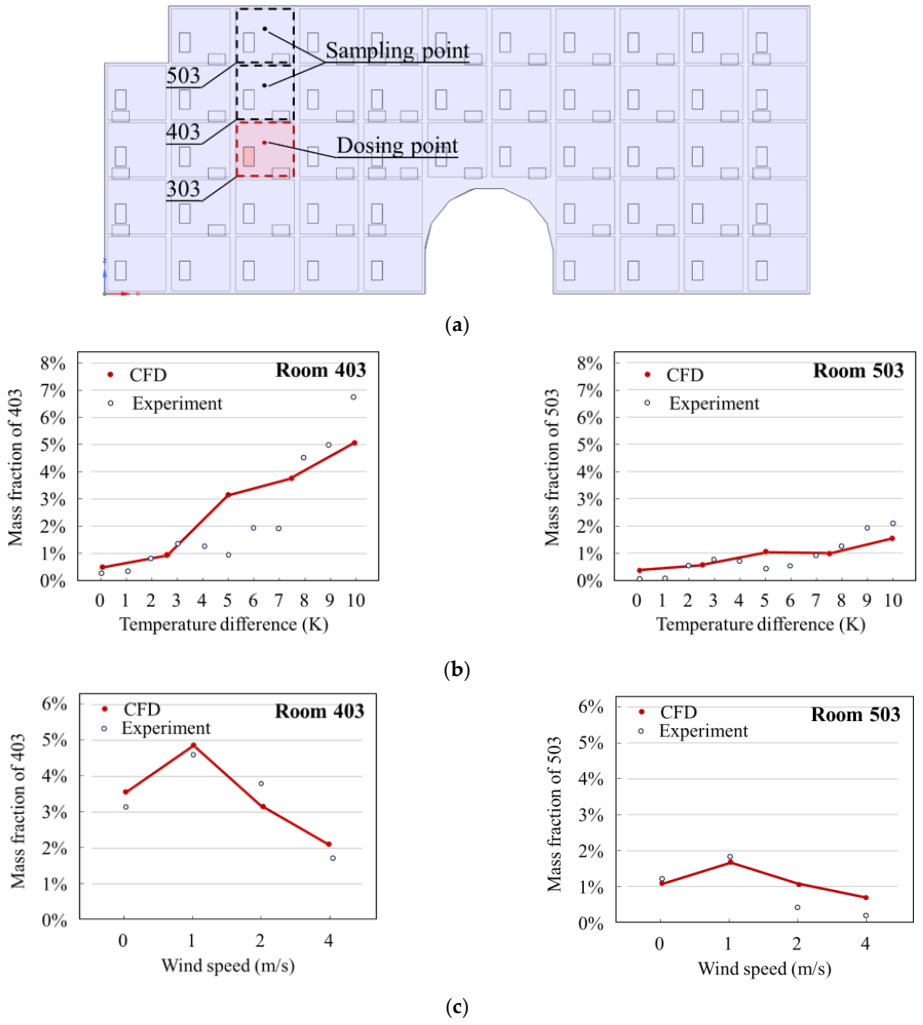

Figure 4. Comparison of the CFD-predicted tracer gas mass fractionwith the experimental data. (**a**) Schematic of the field-tested building; (**b**) the effect of indoor–outdoor temperature difference on the tracer gas mass fraction in the receptor rooms (403 and 503); (**c**) the effect of outdoor wind speed on the tracer gas mass fraction in the receptor rooms (403 and 503).

To quantify the infection risk caused by cross-contamination, the ratio of the air that was expelled from the source room and entered the receptor room was defined as the re-entry ratio (Equation (6)) [11]. This ratio helps in determining the amount of air that is discharged from the source room and then enters the upper floors.

$$k = \frac{C_j (ACH)_j V_j}{C_i (ACH)_i V_i} \tag{6}$$

where C represents the tracer gas concentration in the room, ACH represents the air changes per hour, V represents the volume of the room, and i and j refer to the source room and receptor room, respectively.

Based on the re-entry ratio of air expelled from the source room entering the upper floors, the Wells–Riley equation (Equation (7)) can be used to estimate the infection risk of viral aerosols transmitted through the air [16]. This model has been widely used to assess the risk of airborne transmission. The Wells–Riley model is defined as follows:

$$P = 1 - e^{\frac{-Iqpt}{Q}} \tag{7}$$

where q represents the dose (q = 48), which indicates the infectivity of the pathogen [17]; I represents the initial number of infections (assuming I = 1); p represents the pulmonary ventilation rate (p = 0.6 m^3/h) [11]; t represents the exposure time (set as t = 1 h); Q represents the absolute air exchange rate of the room (m^3/h), which can be calculated from the room volume (V, m^3) and air changes per hour (ACH). According to the ASHRAE Handbook [18], the indoor air exchange rate per hour (ACH) is defined as the gas flow rate Q (m^3/s) divided by the room volume V (m^3), namely $ACH = Q/V$. To assess the infection risk of individuals in the receptor room, the mass fraction (M) of viral aerosols transmitted from the source room to the receptor room should be considered. The mass fraction was first introduced by Niu and Tung [11] and further developed by Ai et al. [19] based on the three-zone airflow and mass balance model to quantitatively assess the airflow between units. The detailed derivation can be found in the literature [11].

M_{i-j} is defined as the mass fraction of air originating from source room i and present in receptor room j, and can be calculated by the following equation:

$$M_{i-j} = \frac{C_j}{C_i} \tag{8}$$

where C_i represents the concentration in the source room and C_j represents the concentration in the receptor room. In this study, based on the tracer gas concentration monitoring in different rooms, the mass fractions $M_{303-402}$, $M_{303-403}$, $M_{303-404}$, and $M_{303-503}$ reflect the transmission of the tracer gas from the source room to the receptor rooms.

By substituting the tracer gas mass fraction M_{i-j} into Equation (7), the infection risk for each room can be calculated using the following equation:

$$P = 1 - e^{\frac{-IM_{i-j}qpt}{Q}} \tag{9}$$

The simulation results were compared with the experimental data. Using wind speed and the indoor–outdoor temperature difference as independent variables, the effects of these factors on the tracer gas mass fractions in different rooms were statistically analyzed (Figure 4b,c). The mass fraction of tracer gas in the receptor room showed a positive correlation with the indoor–outdoor temperature difference, and this phenomenon became more pronounced as the temperature difference increased (Figure 4b). However, for the tracer gas mass fraction in Room 403, the CFD prediction deviated significantly from the experimental data when the temperature difference was 5 K. One possible reason for this discrepancy is that the outdoor wind direction differed from the inlet wind speed used in the simulation. Although the simulation results did not exactly match the experimental data, considering the differences in boundary conditions, the CFD simulation results can still be considered reliable.

3. Results

Since single-sided natural ventilation depends on the airflow near the wall surfaces, the air changes per hour (ACH) in the rooms on each floor will vary with the changes in the attachments on the exterior walls. This study mainly discusses the impact of different exterior wall attachments on the vertical transmission within buildings.

3.1. The Impact of Different Types of Attachments on Pollutant Dispersion

The air changes per hour (ACH) on each floor increase with the floor height (Figure 5). On the first and second floors, the ventilation methods with different types of attachments had a similar effect on the ACH, and the natural ventilation rates were nearly identical. On the third floor, differences between the types began to emerge. The ACH was higher on the

fourth and fifth floors. Among them, the flat facade (FF) type showed the highest average ACH across all floors, reaching 4.50 h^{-1} on the fifth floor, demonstrating the strongest natural ventilation capacity. In contrast, the awning + outdoor unit (AN + OU) type exhibited a lower ACH on each floor. The outdoor unit (OU) type had a significantly lower ACH of 2.16 h^{-1} on the first floor, but its ventilation performance gradually improved with the increasing floor height. On the fourth and fifth floors, the ACH of the outdoor unit (OU) type approached that of the flat facade (FF) type. The performance of the outdoor unit (OU) type on the lower floors was relatively stable, and there was no significant improvement in the ACH. Overall, the flat facade (FF) type offered the best ventilation performance across all floors, making it more suitable for scenarios requiring efficient ventilation. However, under the same conditions, the infection risk in the receptor rooms may be higher in such buildings. On the other hand, the awning + outdoor unit (AN + OU) type performed well in multi-story buildings, and is suitable for scenarios requiring stable ventilation.

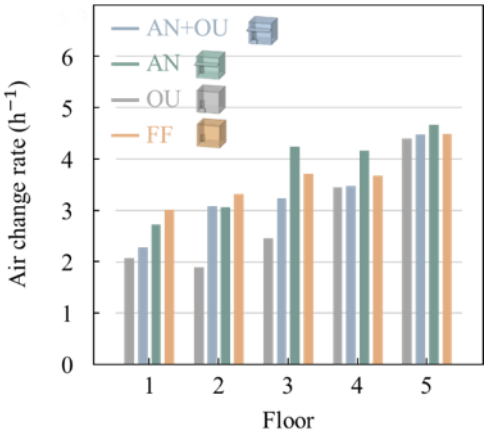

Figure 5. The impact of different building attachments and floor levels on the air exchange rate (AN + OU: awning + outdoor unit, AN: awning, OU: outdoor unit, FF: flat façade).

When the external wall has no attachments (FF), the airflow traversing the wall encounters minimal resistance, leading to an average air change per hour (ACH) of 3.74/h^{-1}. This allows the natural wind to effectively facilitate the air exchange between indoor and outdoor spaces, significantly enhancing the ventilation effect. For awnings (AN), the average ACH was 3.70/h^{-1}. Apart from effectively impeding the vertical transmission of viral aerosols outdoors, they can shield direct sunlight in summer, thereby reducing indoor temperatures and curbing the building energy consumption. Additionally, the awning's presence can modify the wind direction and speed adjacent to the external wall, guiding the natural wind to enter the room at a more advantageous angle, thus increasing the airflow velocity and ventilation volume. Outdoor units (OUs), once installed on the building's external wall, often obstruct the natural wind flow. When an outdoor unit was positioned near ventilation openings, the average indoor ACH dropped from 3.74/h^{-1} to 2.98/h^{-1}. The irregular form of the outdoor unit frequently induces turbulence in the passing airflow, resulting in chaotic air movement that diminishes the airflow's speed and directionality, consequently affecting the ventilation efficiency and quality. The ventilation scenario for the combination of an awning and an outdoor unit (AN + OU) was akin to that of the OU case, with a lower ACH compared with other types. Due to the addition of an outdoor unit to the FF configuration, the overall average ACH was lower than that of the FF, registering at 3.31/h^{-1}.

The distribution of tracer gas mass fractions further elucidated the influence of different external wall attachments on the vertical outdoor transmission of pollutants (Figure 6 and Table 1). When natural wind blows horizontally toward the building, the

inclined angle of the awning can deflect a portion of the airflow upward, thus partially preventing the upward diffusion of contaminated air. In the AN and AN + OU configurations, the awnings on the exterior walls of the source room generated an "air curtain" effect (Figure 6c,d). This air curtain halted the upward spread of contaminated air, confining it to lower floors. As a result, in buildings with AN and AN + OU attachments, the tracer gas mass fractions in receptor rooms, particularly those on the fourth floor, were remarkably reduced. On the fifth floor, the tracer gas mass fractions for the FF, OU, AN, and AN + OU scenarios were 2.7%, 3.8%, 2.5%, and 0.8%, respectively. This indicates that the awning can, to a certain extent, decrease the accumulation of contaminated air on higher floors. The lowest mass fraction was observed in the AN + OU configuration, as the outdoor unit caused the air entering the room to originate more from horizontal airflow rather than predominantly from the lower levels, as was the case with the OU or AN configurations. On the fourth floor, the tracer gas mass fractions in receptor rooms for the FF, OU, and AN scenarios were 10.0%, 9.5%, and 6.9%, respectively. Similarly, the AN configuration exhibited relatively lower mass fractions. Although awnings cannot entirely prevent the upward transmission of viral aerosols due to their structural characteristics, they can mitigate the accumulation of contaminated air on higher floors by altering the natural wind direction and reducing the indoor–outdoor temperature difference. This contributes to reducing the vertical outdoor transmission of pollutants.

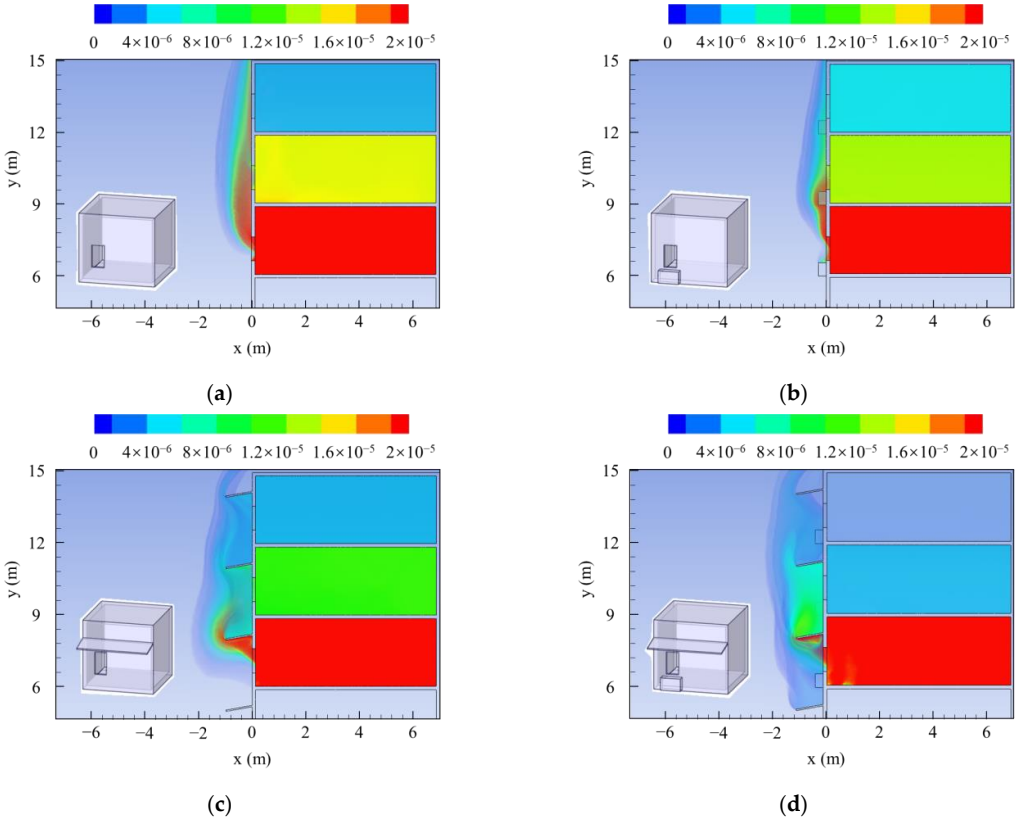

Figure 6. Tracer gas concentration distribution under different external wall attachments. (**a**) FF, (**b**) OU, (**c**) AN, (**d**) AN + OU.

Table 1. Average tracer gas concentration.

Floor	FF	OU	AN	AN + OU
5	2.7%	3.78%	2.5%	0.8%
4	10.0%	9.5%	6.9%	3.1%
3	100.0%	100.0%	100.0%	100.0%

In conclusion, the AN + OU building type demonstrated the optimal performance in controlling pollutant gas transmission. Compared with FF, the tracer gas concentration decreased by an average of 4.4% per floor. Next was AN, which reduced the concentration by 1.6%, while OU increased it by 0.6%.

In order to gain a better understanding of the impact of different attachments on inter-flat pollutant transmission, Figure 7 illustrates the heat flux distribution in the central z-plane for various attachment types. As Shown in Table 2, rooms with the flat facade (FF) and outdoor unit (OU) attachments generally had relatively higher average temperatures, while the average temperature under the awning (AN) condition was relatively lower. The awning + outdoor unit (AN + OU) type featured more uniform average temperatures across different floors. When there are no attachments on the external wall (FF), natural wind can flow relatively smoothly, leading to a more balanced temperature distribution without overly high temperatures. The outdoor unit (OU) type had an impact on the air changes per hour. By observing the airflow direction at the windows, it was noted that the presence of the outdoor unit hindered cold air from entering through the lower part of the window, thus influencing the overall temperature distribution within the room. Compared with the OU scenario, in the AN scenario, the awning blocked some of the hot air from the lower rooms, thereby reducing the increase in indoor temperature. The AN + OU type was more complicated, since its temperature distribution was affected by both the awning and the outdoor unit. This may either lower the temperature due to the blockage of vertical airflow or raise it because of the impact of the outdoor unit on indoor ventilation. Therefore, its average temperature lay between that of AN and OU. All in all, due to the unique shape and function of the awning, the AN type of building could effectively block pollutants coming from below while maintaining a relatively high air change rate (ACH), thus providing a relatively clean air environment indoors.

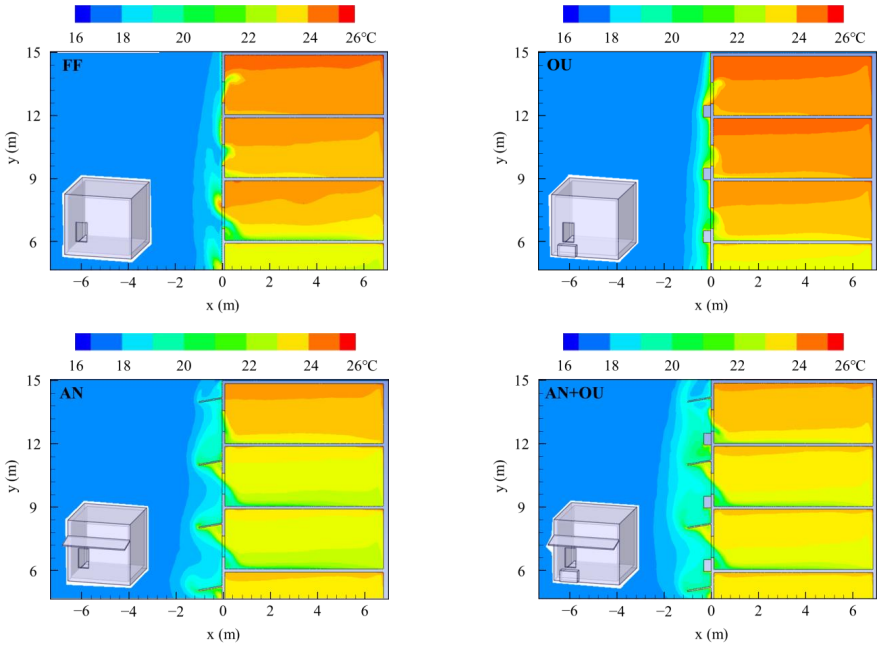

Figure 7. Schematic diagram of the heat flux profile distribution under different external wall attachments.

Table 2. Average temperature of each room.

Floor	FF	OU	AN	AN + OU
5	25.44	25.66	25.25	24.82
4	25.19	25.61	23.87	24.23
3	23.95	25.11	23.72	24.10

3.2. Cross-Contamination Risk Assessment

Under the OU scenario, the hourly infection risk in each receptor room was relatively high (Table 3), with an average infection risk of 2.07%, followed by FF at 1.29%. Due to the lower ACH, OU exhibited the highest infection risk. The average infection risk in receptor rooms under AN was lower than that of FF, at 0.70%. The average infection risk in receptor rooms under AN + OU was the lowest at 0.41%, although the infection risk in the source room was higher.

Table 3. Hourly infection risk in the source room and two receptor rooms.

Room	FF	OU	AN	AN + OU
503	0.59%	1.07%	0.41%	0.21%
403	1.98%	3.07%	1.26%	0.60%
303	13.96%	25.03%	17.02%	20.64%

3.3. The Impact of Awning Length on Pollutant Transmission

When selecting an awning length of 0.5 m, the tracer gas mass fraction in the receptor room was higher than that in the FF-type building (Figure 8. A shorter awning leads to a smaller area of airflow dispersion at the external wall, which increases the concentration mass fraction of pollutants in the airflow entering the upper-floor rooms. As shown in Table 4, when the awning length was 1 m, the tracer gas mass fraction in the receptor room decreased by 27.6% (on the fifth floor) and 33.2% (on the fourth floor) compared with the 0.5 m awning. When the awning length was 1.5 m, the tracer gas mass fraction in the receptor room decreased by only 10.2% (on the fifth floor) and 11.1% (on the fourth floor) compared with the 1 m length. Further increasing the awning length had a limited effect on reducing the infection risk. In summary, an awning length of 1.0 m is most suitable.

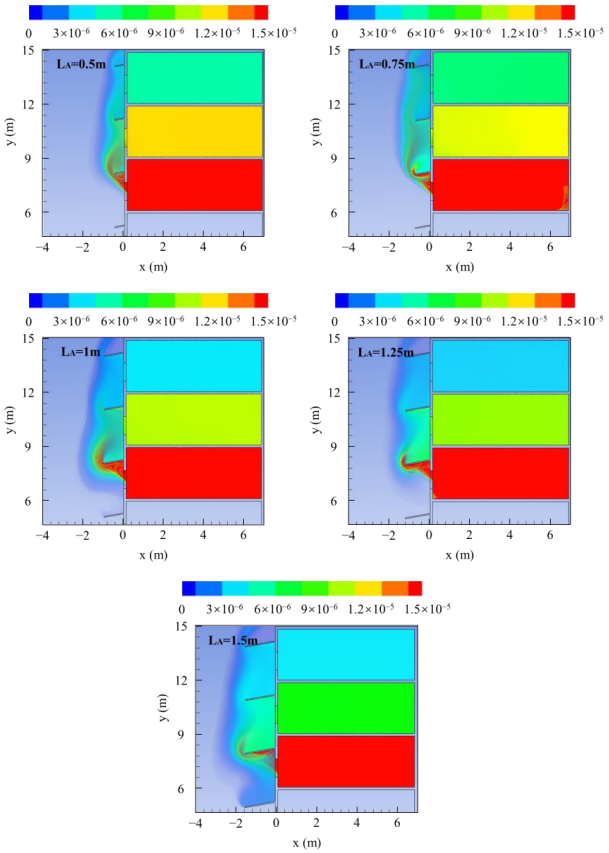

Figure 8. Tracer gas concentration distribution for different awning lengths.

Table 4. The impact of different awning projection lengths on the tracer gas mass fraction in receptor rooms.

L_A	0	0.5	0.75	1	1.25	1.5
5	2.7%	3.5%	3.2%	2.5%	2.4%	2.3%
4	10.0%	10.4%	8.2%	6.9%	6.3%	6.2%
3	100%	100%	100%	100%	100%	100%

4. Discussion

In this study, a building model was established based on an actual isolation hotel, and computational fluid dynamics (CFD) was utilized to explore the inter-flat transmission mechanism of viral aerosols potentially triggered by single-sided natural ventilation. The impact of external wall attachments on the transmission risk under four scenarios, namely no attachments, only outdoor units, only awnings, and the simultaneous installation of both outdoor units and awnings, was quantified. Moreover, a quantitative analysis was conducted to examine how the outdoor wind speed and the indoor–outdoor temperature difference influenced the transmission pathways.

Generally speaking, the presence of an awning tends to reduce the indoor daylighting effect to some extent. During winter, when daylighting decreases, the indoor temperature also drops, which affects the thermal pressure and subsequently influences the ACH in the room. Typically, a lower indoor–outdoor temperature difference may lead to a corresponding reduction in the air changes per hour [20]. Due to the existence of the awning, the "cascade" effect is significantly weakened. The "cascade" effect usually refers to a phenomenon where airflow and heat are transferred layer by layer in the vertical direction in the absence of an awning [11]. However, the awning changes the airflow path and reduces the wind speed in the vertical direction. Wang et al. [21] employed a CFD model to simulate the impact of awning-type external windows on the ACH and concluded that the ventilation rate was the highest when the angle of wind incidence matched the tilt angle of the awning. The main reason for this difference is that when the wind blows directly toward the building's external wall, awning-type windows create a certain obstruction to the airflow, which is consistent with the conclusions of this study. Nevertheless, the presence of an awning may also enhance the gas transmission between rooms on the same side of the same floor. This phenomenon is rather complex, and currently, we speculate that the awning alters the direction and speed distribution of the airflow, causing changes in the pressure difference between rooms on the same floor, thus promoting gas transmission between these rooms. Furthermore, considering the upward vertical transmission effect on the windward side of high-rise buildings, placing high-risk patients in rooms on higher floors may significantly reduce the overall infection risk. However, this hypothesis requires further specific experiments and simulations for verification.

Considering factors such as safety, daylighting, cost, and pollutant transmission, the selection of the awning length is crucial. It should ensure effective isolation while minimizing the impacts on daylighting and safety, and also take cost factors into account. The projection length of the awning affects the vertical outdoor transmission of pathogens. When choosing an awning for isolating pollutant gases, multiple factors such as transmission risk and illumination need to be considered. An appropriately extended awning not only controls the installation cost, but also enhances the indoor thermal comfort [22] while reducing the safety risks due to potential damage to the awning. In strong wind conditions, overly long awnings may be subjected to substantial wind forces, making them more prone to breaking or detaching, which could pose hazards to pedestrians and the building. The length of the awning also influences indoor daylighting; longer awnings block more sunlight, causing the interior to become dimmer and requiring increased artificial lighting, which leads to higher energy consumption. The length and material of the awning directly impact its cost;

longer awnings generally require more materials and higher installation costs, and will also be more expensive to maintain and replace. Shorter awnings are relatively stable, provide better daylighting, and have lower costs, but may not meet the requirements for isolating pollutant gases. Therefore, the use of a 1 m-long awning is recommended to reduce the risk of tracer gas transmission.

The infection risk of the awning + outdoor unit (AN + OU) type was the lowest across all floors. Buildings with both an awning and an outdoor unit usually have more complex airflow at the external wall. The presence of the awning reduces the extent of the upward diffusion of pollutant gases, while the airflow in the horizontal direction (x-direction) ensures adequate ventilation. However, the relatively lower ACH results in fewer pollutant gases entering the room, thus leading to the lowest overall infection risk. Due to the complexity and instability of the outdoor airflow, the related mechanisms should be further investigated and verified through additional experiments.

In the simulation by Wang et al. [12], the wind speed at the boundary condition inlet was set to 0. This setting simplified the simulation conditions to some extent, but it could also introduce a certain degree of deviation from the real-world conditions. In actual environments, the wind speed at the boundary is rarely completely stagnant, and there is usually some airflow. In contrast, in the current simulation, the wind speed at the boundary condition inlet was set to 2 m/s. This setting led to greater fluctuations in indoor temperature, gas concentration, and other data during the simulation. However, these fluctuations more closely reflect the real-world conditions, providing a better representation of how wind in the natural environment affects the internal building environment. Indoor temperature can change due to the outdoor wind speed, and gas concentrations will experience different degrees of diffusion and mixing due to the airflow. Ventilation is one of the most widely used interventions to reduce the indoor infection risk [23–25]. Unilateral natural ventilation can be considered to transform into mechanical ventilation. Although it may be expensive, this ventilation mode can effectively prevent the transmission of viruses near the wall [26]. Exterior wall renovations generally have little significant impact on the indoor energy efficiency, as such attachments basically do not alter the thermophysical properties of the building envelope. Regarding building maintenance, exterior wall renovations, such as adding sunshades, may increase the risk of falling during extreme weather conditions. However, this is inevitable. Shortening the length of the sunshades as much as possible before the arrival of gale-force winds can help to reduce the probability of such hazards.

Based on the research, the following suggestions have been put forward for building codes or guidelines. In the design of building facade attachments, promote the combined configuration of awnings and outdoor units, and standardize the length of awnings to be around 1 m. In terms of ventilation design, when conditions permit, replace single-sided natural ventilation with mechanical ventilation to balance ventilation and the infection risk. Regarding building layout and room allocation, arrange high-risk patients on higher floors, and optimize the room layout and air distribution.

This study had several limitations. First of all, a constant temperature boundary condition was applied to the indoor walls, which may differ from the actual measurements [11,27,28]. However, in another paper [29], a constant wall temperature was also set to simulate convective heat transfer. In the steady-state thermal analysis of a multi-layer wall, the temperature boundary conditions of the inner and outer surfaces of the wall were set based on the coldest day of the past winter in Mishkolc, Hungary, where the temperature of the inner surface was 22 °C (295 K). The outer surface temperature was −8 °C (265 K). Although this simplification helped to streamline the simulation conditions, it inevitably introduced some errors in the calculated air change rate compared with the real-world scenarios. Second, this study only considered the impact of the outdoor unit

under static conditions on the airflow. While this approach partially reflected the effect of the outdoor unit on the surrounding airflow, it ignored the disturbance generated by the fan when the outdoor unit was operating. When the outdoor unit was turned on, the rotation of the fan generated strong airflow, which may have significantly affected the vertical transmission. Finally, although the fluctuations in the data may have increased the complexity of the analysis, they provided simulation results that were closer to the real-world conditions, helping to more accurately understand and assess the impact of various factors on the internal building environment.

5. Conclusions

1. The mass fraction of the tracer gas in the receptor room was positively correlated with the indoor–outdoor temperature difference. As the temperature difference increases, the mass fraction also increases. When the outdoor wind speed increased, the mass fraction first increased and then decreased, which was the result of the combined effect of buoyancy and wind force.
2. In terms of the ACH, the flat facade (FF) type had the best ventilation performance, followed by the awning (AN) type and the awning + outdoor unit (AN + OU) type.
3. In terms of the infection risk, the flat facade (FF) type had a relatively high infection risk, with an average hourly infection risk of 1.29% in the receptor room; the outdoor unit (OU) type had the highest infection risk (2.07%) due to the low ACH; the awning (AN) type had a lower infection risk of 0.7%; and the awning + outdoor unit (AN + OU) type had the lowest overall infection risk at 0.41%.
4. The selection of the awning length is crucial. When the length was 0.5 m, the isolation effect was not ideal, while a length of 1 m was more suitable. Further increases in length resulted in a limited reduction in the infection risk.

Author Contributions: Conceptualization, N.Z.; Methodology, Y.L. and N.Z.; Software, N.Z.; Validation, Y.L. and N.Z.; Formal analysis, Y.L. and Y.J.; Investigation, Y.L., Y.J. and X.L.; Resources, N.Z.; Data curation, Y.L. and N.Z.; Writing—original draft preparation, Y.L.; Writing—review and editing, Y.L. and N.Z.; Visualization, Y.L. and N.Z.; Supervision, N.Z.; Project administration, N.Z.; Funding acquisition, N.Z. All authors have read and agreed to the published version of the manuscript.

Funding: This work was supported by the National Natural Science Foundation of China (grant number: 52478074).

Institutional Review Board Statement: This experiment was authorized by the Ethics Committee of Beijing University of Technology (No. CJXB11).

Data Availability Statement: The original details of the data presented in this study are available upon request from the corresponding author.

Conflicts of Interest: The authors declare no conflicts of interest.

References

1. Jordan-Martin, N.C.; Madad, S.; Alves, L.; Wang, J.; O'Gere, L.; Smith, Y.G.; Pressman, M.; Shure, J.A.; Cosmi, M. Isolation hotels: A community-based intervention to mitigate the spread of the COVID-19 pandemic. *Health Secur.* **2020**, *18*, 377–382. [CrossRef] [PubMed]
2. Cheng, P.; Chen, W.; Xiao, S.; Xue, F.; Wang, Q.; Chan, P.W.; You, R.; Lin, Z.; Niu, J.; Li, Y. Probable cross-corridor transmission of SARS-CoV-2 due to cross airflows and its control. *Build. Environ.* **2022**, *218*, 109137. [CrossRef] [PubMed]
3. Li, Y.; Qian, H.; Hang, J.; Chen, X.; Cheng, P.; Ling, H.; Wang, S.; Liang, P.; Li, J.; Xiao, S. Probable airborne transmission of SARS-CoV-2 in a poorly ventilated restaurant. *Build. Environ.* **2021**, *196*, 107788. [CrossRef] [PubMed]
4. Wong, S.C.; Chen, H.; Lung, D.C.; Ho, P.L.; Yuen, K.Y.; Cheng, V.C.C. To prevent SARS-CoV-2 transmission in designated quarantine hotel for travelers: Is the ventilation system a concern? *Indoor Air* **2021**, *31*, 1295. [CrossRef]

5. Li, X.; Chen, H.; Lu, L.; Chen, L.-L.; Chan, B.P.-C.; Wong, S.-C.; Cheng, V.C.-C.; Yuen, K.-Y.; Chan, K.-H.; To, K.K.-W. High compliance to infection control measures prevented guest-to-staff transmission in COVID-19 quarantine hotels. *J. Infect.* **2022**, *84*, 418. [CrossRef] [PubMed]
6. Grout, L.; Katar, A.; Ait Ouakrim, D.; Summers, J.A.; Kvalsvig, A.; Baker, M.G.; Blakely, T.; Wilson, N. Failures of quarantine systems for preventing COVID-19 outbreaks in Australia and New Zealand. *Med. J. Aust.* **2021**, *215*, 320–324. [CrossRef] [PubMed]
7. Wu, S.-S.; Zhang, J.-J.; Sun, Y.; Ren, Z.-Y.; Dou, X.-F.; Zhang, L.; Duan, W.; Ma, C.; Yang, P.; Pang, X. Survey of possible aerosol transmission of a COVID-19 epidemic caused by 2019-nCoV delta variant. *Zhonghua Liu Xing Bing Xue Za Zhi = Zhonghua Liuxingbingxue Zazhi* **2022**, *43*, 305–309. [PubMed]
8. Linden, P.F. The fluid mechanics of natural ventilation. *Annu. Rev. Fluid Mech.* **1999**, *31*, 201–238. [CrossRef]
9. Zhang, G.; Li, L.; Yu, Y.; Liu, J.; Zhang, Q. Thermal Resilience of Public Building Atriums Under Different States During Heatwaves. *Buildings* **2025**, *15*, 598. [CrossRef]
10. Liu, X.; Niu, J.; Gao, N.; Perino, M.; Heiselberg, P. CFD simulation of inter-flat air cross-contamination—A possible transmission path of infectious diseases. In Proceedings of the 10th International Building Performance Simulation Association Conference and Exhibition, Building Simulation 2007, Beijing, China, 3–6 September 2007.
11. Niu, J.; Tung, T. On-site quantification of re-entry ratio of ventilation exhausts in multi-family residential buildings and implications. *Indoor Air* **2008**, *18*, 12–26. [CrossRef] [PubMed]
12. Wang, J.; Zhang, T.; Wang, S.; Battaglia, F. Gaseous pollutant transmission through windows between vertical floors in a multistory building with natural ventilation. *Energy Build.* **2017**, *153*, 325–340. [CrossRef] [PubMed]
13. Partankar, S. *Numerical Heat Transfer and Fluid Flow*; Hemisphere Publishing Corporation: Washington, DC, USA, 1980.
14. Zhang, T.; Li, P.; Zhao, Y.; Wang, S. Various air distribution modes on commercial airplanes—Part 2: Computational fluid dynamics modeling and validation. *HVAC&R Res.* **2013**, *19*, 457–470.
15. Jiang, Y.; Chen, Q. Buoyancy-driven single-sided natural ventilation in buildings with large openings. *Int. J. Heat Mass Transf.* **2003**, *46*, 973–988. [CrossRef]
16. Riley, E.; Murphy, G.; Riley, R. Airborne spread of measles in a suburban elementary school. *Am. J. Epidemiol.* **1978**, *107*, 421–432. [CrossRef] [PubMed]
17. Dai, H.; Zhao, B. Association of the infection probability of COVID-19 with ventilation rates in confined spaces. *Build. Simul.* **2020**, *13*, 1321–1327. [CrossRef] [PubMed]
18. American Society of Heating, Refrigerating and Air-Conditioning Engineers (ASHRAE). *2009 ASHRAE Handbook: Fundamentals*; ASHRAE: Atlanta, GA, USA, 2009; Volume 1.
19. Ai, Z.; Mak, C.M.; Niu, J. Numerical investigation of wind-induced airflow and interunit dispersion characteristics in multistory residential buildings. *Indoor Air* **2013**, *23*, 417–429. [CrossRef]
20. Wallace, L.; Emmerich, S.J.; Howard-Reed, C. Continuous measurements of air change rates in an occupied house for 1 year: The effect of temperature, wind, fans, and windows. *J. Expo. Sci. Environ. Epidemiol.* **2002**, *12*, 296–306. [CrossRef] [PubMed]
21. Wang, H.; Karava, P.; Chen, Q. Development of simple semiempirical models for calculating airflow through hopper, awning, and casement windows for single-sided natural ventilation. *Energy Build.* **2015**, *96*, 373–384. [CrossRef]
22. Rossi, F.; Cardinali, M.; Gambelli, A.M.; Filipponi, M.; Castellani, B.; Nicolini, A. Outdoor thermal comfort improvements due to innovative solar awning solutions: An experimental campaign. *Energy Build.* **2020**, *225*, 110341. [CrossRef]
23. Song, Y.-W.; Kim, S.-E.; Park, J.-C. Indoor Air Pollutant (PM 10, CO_2) Reduction Using a Vortex Exhaust Ventilation System in a Mock-Up Room. *Buildings* **2025**, *15*, 144. [CrossRef]
24. Zhang, H.; Zhao, P.; Dou, Z.; Su, B.; Li, Y.; Zhang, N. Transmission of respiratory diseases in high-metabolic environments: A case study of gym. *Build. Environ.* **2024**, *267*, 112161. [CrossRef]
25. Xu, Z.; Zhang, H.; Zhu, M.; Ji, Y.; Xue, P.; Xie, J.; Li, Y.; Zhang, N. Human behavior-based COVID-19 transmission in two dining spaces. *J. Hazard. Mater.* **2024**, *480*, 135820. [CrossRef] [PubMed]
26. Zhang, N.; Liu, X.; Gao, S.; Su, B.; Dou, Z. Popularization of high-speed railway reduces the infection risk via close contact route during journey. *Sustain. Cities Soc.* **2023**, *99*, 104979. [CrossRef]
27. Wu, Y.; Tung, T.C.; Niu, J. Experimental analysis of driving forces and impact factors of horizontal inter-unit airborne dispersion in a residential building. *Build. Environ.* **2019**, *151*, 88–96. [CrossRef]
28. Wu, Y.; Tung, T.C.; Niu, J.-L. On-site measurement of tracer gas transmission between horizontal adjacent flats in residential building and cross-infection risk assessment. *Build. Environ.* **2016**, *99*, 13–21. [CrossRef]
29. Omle, I.; Askar, A.H.; Kovács, E. Optimizing the Design of Container House Walls Using Argon and Recycled Plastic Materials. *Buildings* **2024**, *14*, 3944. [CrossRef]

Disclaimer/Publisher's Note: The statements, opinions and data contained in all publications are solely those of the individual author(s) and contributor(s) and not of MDPI and/or the editor(s). MDPI and/or the editor(s) disclaim responsibility for any injury to people or property resulting from any ideas, methods, instructions or products referred to in the content.